Lateral Diffusion Length Changes in HgCdTe Detectors in a Proton Environment

John E. Hubbs, *Member, IEEE,* Paul W. Marshall, *Member, IEEE,* Cheryl J. Marshall, *Member, IEEE,* Mark E. Gramer, Diana Maestas, John P. Garcia, Gary A. Dole, and Amber A. Anderson,

***Abstract*— This paper presents a study of the performance degradation in a proton environment of very long wavelength infrared (VLWIR) HgCdTe detectors. The energy dependence of the Non-Ionizing Energy Loss (NIEL) in HgCdTe provides a framework for estimating the responsivity degradation in VLWIR HgCdTe due to on orbit exposure from protons. Banded detector arrays that have different detector designs were irradiated at proton energies of 7, 12, and 63 MeV. These banded detector arrays allowed insight into how the fundamental detector parameters degraded in a proton environment at the three different proton energies. Measured data demonstrated that the detector responsivity degradation at 7 MeV is 5 times larger than the degradation at 63 MeV. The comparison of the responsivity degradation at the different proton energies suggests that the atomic Columbic interaction of the protons with the HgCdTe detector is likely the primary mechanism responsible for the degradation in responsivity at proton energies below 30 MeV.**

***Index Terms*— HgCdTe detectors, Proton radiation effects, Non-Ionizing Energy Loss (NIEL)**

I. Introduction

SPACE based infrared imaging systems place stringent performance requirements on very long wavelength infrared (VLWIR) detectors in terms of sensitivity, uniformity, operability, and radiation hardness. The radiation hardness goals for space based imaging systems are typically dominated by proton interactions with the FPA. The three sources of protons for space-based detectors include (1) protons in the inner Van Allen radiation belt, (2) the proton component of solar particle events and (3) hydrogen nuclei from intergalactic cosmic rays. Interaction of the protons with the HgCdTe detectors results in permanent performance degradation primarily due to total ionizing dose (TID) effects and displacement damage effects. The TID effects are generated by the loss of the kinetic energy from an incident proton to ionization and primarily degrade the operation of readout integrated circuits (ROIC) through flat-band voltage shifts and increased leakage currents. Displacement damage effects result when a small amount of the proton energy is lost to non-ionizing processes causing atoms to be removed from their lattice sites and form permanent electrically active defects. These displacement damage effects primarily degrade the performance of the HgCdTe detector array through increased dark current, reduction in responsivity, and degraded uniformity.

Recent radiation results from VLWIR HgCdTe detector arrays[1] have shown a change in responsivity and lateral collection with increasing proton fluence. These measured data exhibit an exponential decrease in responsivity with increasing proton fluence. This loss in responsivity has been isolated to the detector, and its root cause is related to the detector design, which relies on lateral collection of charge to achieve high performance in quantum efficiency. It is this reliance on lateral collection that causes the loss of responsivity in a proton environment. For this detector structure, a major consideration in the design is the diameter of the lateral collection diode implant, which directly affects the noise, responsivity, sensitivity, operability, and tolerance to proton fluence. If the diode diameter is large, the responsivity (detector quantum efficiency) will be maximized, but the operability is degraded due to the increased probability of intersecting a defect. Additionally, when the diode diameter is large, the detector relies less on lateral collection of charge and is more tolerant to interactions with protons. At the other extreme with a small lateral collection diode, the operability of the detector array will be optimized but the responsivity, and consequently the sensitivity, is degraded. Since a detector with a small implant diameter requires a long lateral collection length to achieve reasonable responsivity (quantum efficiency), its performance will degrade if the lateral collection length is compromised in a proton environment. Thus, for this type of detector design, a trade space exists that balances the responsivity and sensitivity performance against operability and proton fluence performance.

This study investigates the change in responsivity and lateral collection length of VLWIR HgCdTe detector in a proton environment with the goal to obtain data to support the development of an on-orbit performance estimation tool for these detector arrays. This analysis assumes that the dominant source of detector performance change is due to displacement

Manuscript received July 1, 2007. This work was supported in part by the Space Vehicles Directorate of the United States Air Force Research Laboratory and the NASA Electronic Parts and Packaging Program (NEPP).

The authors are with Ball Aerospace & Technologies Corp., Albuquerque, NM 87185 USA. (505-846-6627; fax: 505-846-4993; e-mail: jhubbs@ieee.org).

P.W. Marshall is a Consultant, Brookneal, VA 24528 USA. (e-mail: pwmarshall@aol.com).

C.J. Marshall is with the NASA Goddard Space Flight Center, Greenbelt, MD 20771 USA. (email: cmarshal2@aol.com).

A.A. Anderson is with the Space Vehicles Directorate of the Air Force Research Laboratory (AFRL/VSSS) Kirtland AFB, NM 87117 USA. (e-mail: amber.anderson@kirtland.af.mil).

damage resulting from the interaction of protons and the HgCdTe detectors. This estimation tool will utilize the concept of non-ionizing energy loss rate (NIEL) in HgCdTe, which occurs by Coulombic, nuclear elastic, and nuclear inelastic interactions between the protons and the HgCdTe detector material. The energy dependence of the NIEL in HgCdTe provides a framework for estimating the on orbit change in detector responsivity. This model development assumes that displacement damage is linear with proton fluence and that damage in the detectors has the same energy dependence as NIEL—assumptions that will be validated by measurements in this study.

The detectors utilized in this study are banded VLWIR HgCdTe detector arrays with varying diameters of single implant lateral collection diode designs. These banded detector arrays allow insight into how the fundamental detector parameters degrade in a proton environment. For these experiments, the proton response of the banded detector arrays was measured at proton energies of 7, 12, and 63 MeV.

II. Non-ionizing Energy Loss (NIEL) Concept

A goal of this study is to obtain the required data and to perform the necessary analysis to support the development of an on-orbit performance estimation tool for VLWIR HgCdTe detector arrays. This on-orbit performance estimation tool will utilize the concept of non-ionizing energy loss rate (NIEL) in HgCdTe. NIEL is that part of the proton energy introduced to the HgCdTe detector via Coulombic, nuclear elastic, and nuclear inelastic interactions. The energy dependence of the NIEL in HgCdTe provides a framework for estimating the on orbit change in detector responsivity. This section provides background information about NIEL and how it is used to develop on-orbit performance predictions.

In this section, the methods used to compute the proton NIEL in HgCdTe, are briefly described. This methodology follows the treatment initially presented on calculating the NIEL for short-wave and mid-wave detectors[2]. The proton NIEL was calculated for Hg, Cd, and Te and the results were used to obtain the NIEL for the compound material by adding the results for the individual elements weighted by their stoichiometric ratios. NIEL has two components: 1) atomic Coulombic interactions, and 2) nuclear interactions. Atomic scattering tends to dominate at the lower energies while nuclear collisions begin to take over near 30 to 50 MeV.

A. Atomic Coulombic Interactions

The classical Rutherford scattering formula has been widely used for computing the Coulomb contribution to proton NIEL. However, the straightforward application of the classical formulation over the entire energy range, from displacement thresholds to 1 GeV, is not appropriate for the proper evaluation of NIEL. This is particularly true in the low energy region, where a screening potential should be used and in the high energy region where a relativistic treatment of the scattering process is more appropriate. The Ziegler, Biersack, Littmark (ZBL) screened Coulomb potential[3],[4], coupled to the relativistic energy transfer cross sections at higher incident energies[5] was used to correct the classical Coulomb scattering cross section. These corrections are most evident at the lowest and highest energies.

B. Nuclear Interactions

A method to compute the nuclear contribution to the proton NIEL, based on the thin target approximation, using the MCNPX charged particle transport code[6], has been formulated[7]. A thin cylindrical slab of the material of interest with a normalized density of 0.01 atoms/barn-cm was modeled for a pencil beam of protons penetrating the material. The model considers a simulated pencil beam of protons normally incident on a thin, solid cylindrical disk. Using the damage energy tally that is provided as an output from the MCNPX code, the results were analyzed to calculate the mean damage energy per source particle, T_{Dam}, which is the non-ionizing portion of energy deposited (i.e. after application of the Lindhard partition function). Then, NIEL is calculated by:

$$S_{NIEL} = \left(\frac{N}{A}\right)\frac{T_{dam}}{(N_v \cdot x)} \quad (1)$$

where N is Avogadro's number, A is the gram atomic weight of the target material, N_v is the atom density and x is the target thickness. The nuclear contributions to the proton NIEL were computed for each material using MCNPX and these results were used to obtain the NIEL for the compound material by adding the results for the individual elements weighted by their stoichiometric ratios. The results of these calculations are shown in Fig. 1 that shows the separate contributions from nuclear elastic and inelastic interactions as well as the atomic Coulombic interactions. The production of displaced atoms is dominated by the Coulombic interactions below 10 MeV, while the nuclear collisions (particularly the nuclear inelastic) take over at energies above 30 to 50 MeV.

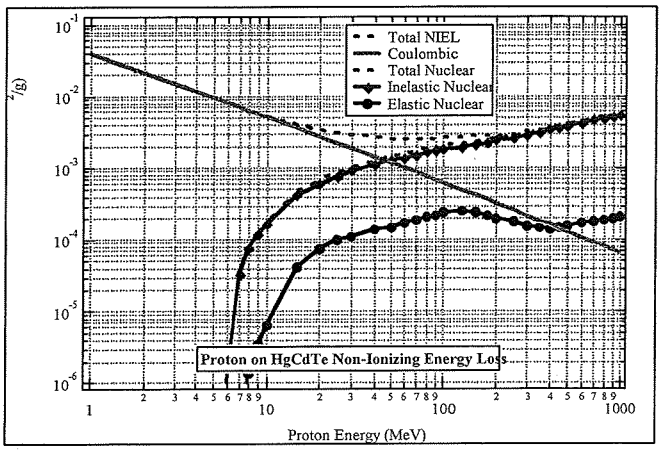

Fig. 1. Non-ionizing Energy Loss for Protons on HgCdTe.

C. Implications Of NIEL Trends For Change in Performance In HgCdTe Detectors

There are two primary aspects of the damage that may be expected to correlate with the calculated proton induced NIEL. The first is the dependence of damage induced detector performance change as a function of proton energy, which

results in a reduction in the lateral collection length leading to a change in detector responsivity. Numerous studies have shown the importance of understanding the energy dependence of damage as a key to relating the measured damage factors in the laboratory at a few discrete energies to the expected detector response to an orbital spectrum of proton energies[8]. The second aspect is the detector-to-detector variations in dark current. NIEL calculations can be extended to look at the second moment of non-ionizing energy deposition and examined to describe this problem in terms of variations in the deposited damage energy[9].

The importance of the inelastic contributions to the NIEL at higher proton energies has implications beyond the expected trends in the damage factors. Inelastic damage results from interactions that occur much less frequently than the atomic Coulombic damage mechanism that dominates at lower proton energies; however, individual inelastic damage events may exceed the average Coulombic interaction by orders of magnitude. For an array of detectors, this suggests that the variation of damage from detector to detector may be dominated by the inelastic interactions. Because of the importance of such inelastic interactions in HgCdTe, detector-to-detector variations in damage induced dark currents could be significant. The analysis of the dark current distribution characteristics for VLWIR HgCdTe detectors in a proton environment is complicated because the pre-radiation dark current distribution are dominated by the HgCdTe material and can mask the effects of the proton radiation.

III. Experiment

A. Description of VLWIR HgCdTe Detector

The VLWIR HgCdTe detectors were grown by molecular-beam epitaxy (MBE) on CdZnTe substrates using a double-layer planar buried heterostructure (DLPH) p-on-n design. The detectors are single implant lateral collection diode designs, with the implant centered in the pixel, coupled with a micro-lens structure as shown in Fig 2.

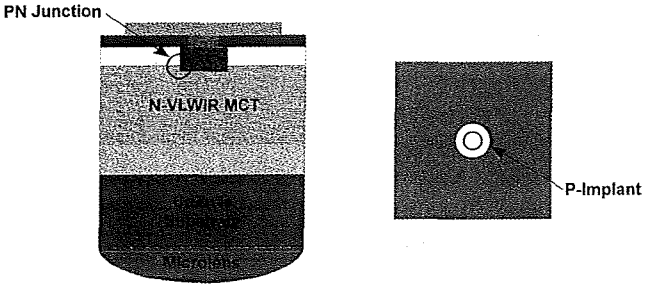

Fig. 2. VLWIR HgCdTe Detector Structure.

This detector design approach is used to improve the RoA and operability of the detector array. The detector arrays are anti-reflection (AR) coated to improve the quantum efficiency at long wavelengths. The VLWIR HgCdTe detector array has a cut-off wavelength of 14.0 μm. Details of the DLPH detector design, the application of lateral collection concepts in DLPH detectors, and the application of microlens technology to VLWIR HgCdTe detectors have been previously described[10], [11], [12], [13]. The detector arrays used in this study are banded to incorporate several different single implant lateral collection diode designs into a single detector array. In this case, the principal design variation for the detector diodes is the diameter of the single implant, which varied from 14 to 46 μm, as shown in Fig. 3. Banded detector arrays are used to help select the optimal detector design for a given pixel size by evaluating the trade-off of lateral collection diode implant diameter versus operability. If the diode diameter is large, the detector responsivity (quantum efficiency) and responsivity uniformity will be maximized at the expense of degraded operability. At the other extreme, a small lateral collection diode offers improved operability and high detector R_0A at the expense of lower responsivity, lower sensitivity, and degraded uniformity.

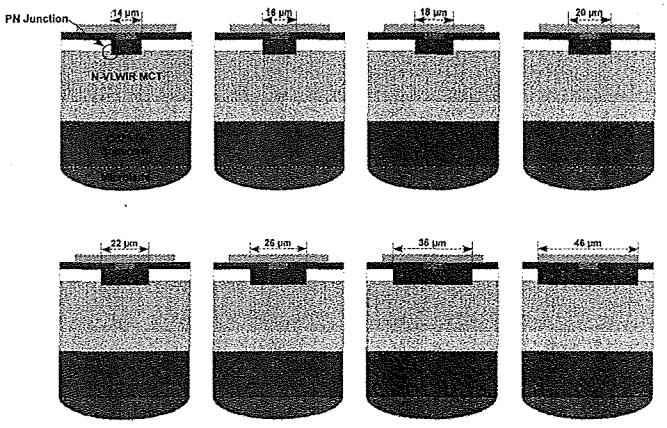

Fig. 3. Banded Array Detector Description.

A finite element model of VLWIR HgCdTe DLPH detectors has been developed[14] to predict the detector responsivity as a function of the minority carrier lateral collection length. This model incorporates several of the design features of the lateral collection detectors including the micro-lens structure. This model also allows the impact of changes in the minority carrier lateral collection length on the detector quantum efficiency, spectral response and other performance parameters to be evaluated. The output from the model consists of the detector responsivity (normalized to responsivity of the detector with the largest implant), as a function of implant diameter. This model permits the performance impact that results from changes in the implant diameter and lateral collection length (LD) to be evaluated. Modeling results indicate that as the implant diameter decreases, the detector responsivity decreases. This model also demonstrates that the detector responsivity has an approximate exponential dependence on the lateral collection length. These modeling results provide insight into the damage mechanism in a proton radiation environment.

B. Proton Irradiation

VLWIR HgCdTe IRFPAs were irradiated at three proton energies of 7, 12, and 63 MeV. The detector arrays were

operated at 40 K and subjected to a series of six proton irradiations to achieve total ionizing dose levels of 10, 20, 50, 100, 200 and 300 krad(Si). After each proton irradiation, the detector array was radiometrically characterized to determine the responsivity of each detector design.

C. Experiment Design

The VLWIR HgCdTe detectors under study collect charge from both the implanted area of each detector as well as from a volume of material around the implant by means of lateral collection. The active detector area is a combination of the implant diameter and the lateral collection length as given by:

$$A_{Det} = \pi\left(r + L_D\right)^2 \quad (2)$$

where r is the radius of the circular implant and L_D is the lateral collection length. The detector signal current is then determined by:

$$i = q\eta E_q A_{Det} = q\eta E_q \pi\left(r + L_D\right)^2 \quad (3)$$

where q is the electron charge (C), η is the detector quantum efficiency, E_q is the photon irradiance at the detector and A_{Det} is the active detector area. For any lateral collection length, the percentage of charge collected in this manner will be larger for smaller implant diameters making the responsivity from the smaller implants more sensitive to changes in the lateral collection length. In a proton environment, the lateral collection length will likely degrade due to a decrease in the minority carrier lifetime with increasing proton radiation fluence, causing a decrease in the volume of the detector material from which charge can be collected. The detector responsivity will degrade in a proton environment because both the effective area and pixel thickness are decreased.

The lateral collection length is typically determined by measuring the photo-generated signal from the variable area detector as a function of detector area. The lateral collection length is then determined from these data by plotting the square root of the detector current, ($\sqrt{i}$), as a function of the detector implant diameter (r), fitting a straight line to the measured data that extends to the abscissa. The lateral collection length is where the fitted line intersects the abscissa. This is a common technique used in evaluating material quality of infrared detectors; however, it does not strictly apply to these detectors.

This type of analysis is complicated for these detectors because of the micro-lens incorporated into the detector structure. Flood illumination is assumed in the analysis; however, the micro-lens tends to focus the light onto the center of the detector structure with a spot size of approximately 25 to 40 μm. The exact value of the spot size is dependent on the wavelength of light and the F/# of the micro-lens. A further complication arises due to the limited extent of the pixels. If the sum of the lateral collection length and the radius of the implant extend beyond the extent of the pixel boundary, this analysis yields incorrect results. To mitigate these complications, the VLWIR HgCdTe DLPH detector finite element model is used to estimate the lateral collection length.

The detector responsivity, which is directly related to the detector quantum efficiency, is measured for several detector implant diameters at each proton fluence. The corresponding lateral collection length is determined from the VLWIR HgCdTe DLPH detectors finite element model. The relative responsivity versus lateral collection diode implant diameter is plotted for a number of different lateral collection lengths for a banded detector array with a pre-radiation lateral collection length of approximately 18 μm. using both the finite element model output and measured data. The measured data is in close agreement with the model prediction. The pre-radiation lateral collection length for these VLWIR HgCdTe detectors is reported[15] to be in the range of 15 to 20 μm. Independent measurement of the lateral collection length validates this pre-radiation value[1]. As previously described, it is difficult to determine the absolute lateral collection length from the measured responsivity versus implant diameter data from the banded detector arrays because of (1) the interaction between the micro-lens array and the lateral collection diodes, and (2) the limited extent of the pixels. It is important to note that this analysis will show the change of the lateral collection length as a function of proton fluence but will not provide an absolute measure of its value.

1) Damage Constants and Factors

The change in the performance of the VLWIR HgCdTe detector in a proton environment is characterized by defining a damage constant, or a damage factor. The damage constant describes the change in fundamental material parameters produced by a given fluence at a given energy. Damage factors are similar except they characterize the observed radiation degradation of a detector performance parameter such as responsivity or sensitivity. For this analysis, damage constants/factors for the lateral collection length and 14 μm implant detector responsivity are reported. It should be noted that the responsivity damage factors and the lateral collection length damage constant should have similar energy dependencies.

a) Lateral Collection Length Damage Constant

The lateral collection length damage factor can be computed from the measured lateral collection length as a function of proton fluence data. The lateral collection length is given by $L = \sqrt{D\tau}$ where D is the diffusion constant and τ is the minority carrier lifetime. The lateral collection length is related to the incident proton fluence by:

$$\frac{1}{L^2} = \frac{1}{L_0^2} + K_L \Phi_P \quad (4)$$

where L_0 is the pre-radiation lateral collection length, K_L is the lateral collection length damage constant, and Φ_P is the proton fluence. The lateral collection length damage constant is determined from the slope of the line formed by plotting the

inverse of the square of the measured lateral collection length versus proton fluence data. This procedure is repeated at each of the measured proton energies of 7, 12, and 63 MeV and the resulting damage factors are correlated with the NIEL energy dependence.

b) Responsivity Damage Factor

The responsivity damage factor, which is the change in responsivity per unit proton fluence, can be computed from the measured responsivity as a function of proton fluence. The change in responsivity is related to the incident proton fluence by:

$$\Delta Responsivity(E) = K_R(E)\Phi_P(E) \quad (5)$$

where $K_R(E)$ is the responsivity damage factor, and Φ_P is the proton fluence. Responsivity damage factors are computed for the 14 μm implant diameter detectors.

The responsivity damage factor is scaled to NIEL using a constant, R, which has units of responsivity change per unit of non-ionizing energy deposited as given by:

$$K_R(E) = R \cdot NIEL(E) \quad (6)$$

2) Performance Predictions Based on Measured Damage Factors

a) Lateral Collection Length On-Orbit Performance

The change in the on-orbit detector lateral collection length can be calculated by knowledge of the proton energy spectrum at the IRFPA, which is typically found by transporting a proton spectrum at a given orbit through spacecraft shielding. The resultant proton spectrum at the detector is integrated with the energy dependence of the NIEL. The result of this calculation is then scaled to convert the NIEL energy dependence to the proper units of the damage constant. This process is given by:

$$\Delta\left(\frac{1}{L_D^2}\right) = \int_{E_1}^{E_2} K_L(E)\frac{d\Phi(E)}{dE}dE = L\int_{E_1}^{E_2} NIEL(E)\frac{d\Phi(E)}{dE}dE \quad (7)$$

where $K_L(E)$ is the energy dependence of the lateral collection length damage function, $\frac{d\Phi(E)}{dE}$ is the differential proton spectrum, NIEL(E) is the energy dependence of the NIEL in HgCdTe in units of $\frac{MeV\text{-}cm^2}{g}$, and L is the scaling factor between NIEL and the lateral collection length damage constant. This analysis assumes that displacement damage is linear with proton fluence and that damage in the detectors has the same energy dependence as NIEL.

b) Responsivity On-Orbit Performance

The change in the on-orbit detector responsivity can be calculated by integrating the product of proton energy spectrum at the detector and responsivity damage factor. The result of this calculation is then scaled to convert the NIEL energy dependence to the proper units of the responsivity damage factor. This process is described by:

$$\Delta Responsivity = \int_{E_1}^{E_2} K_R(E)\frac{d\Phi(E)}{dE}dE = R\int_{E_1}^{E_2} NIEL(E)\frac{d\Phi(E)}{dE}dE \quad (8)$$

where $K_R(E)$ is the energy dependence of the responsivity damage factor, and R is the scaling factor between NIEL and the responsivity damage factor.

IV. EXPERIMENTAL RESULTS AND ANALYSIS

A. Banded Detector Array Responsivity Characteristics versus Implant Diameter

The measured detector responsivity as a function of implant diameter for the banded detector array is shown in Fig. 5. These data demonstrate that the measured responsivity is approximately an exponential function of the implant diameter and varies by 20% from the smallest to the largest implant diameter. The detector array responsivity operability and the uncorrected responsivity non-uniformity (sigma/mean) as a function of implant diameter is shown in Fig. 6. The responsivity operability data demonstrate that the optimal implant diameter for this pixel pitch is in the range of 20 to 30 μm. The operability falls off at large implant diameters because the probability of the implant intersecting a killer defect increases with implant diameter. These data illustrate the trade-off that occurs between performance and operability and show that the detector design with larger diameter implants have higher overall responsivity; however, the detector design with the smaller implants, in general, have a higher number of operable detectors.

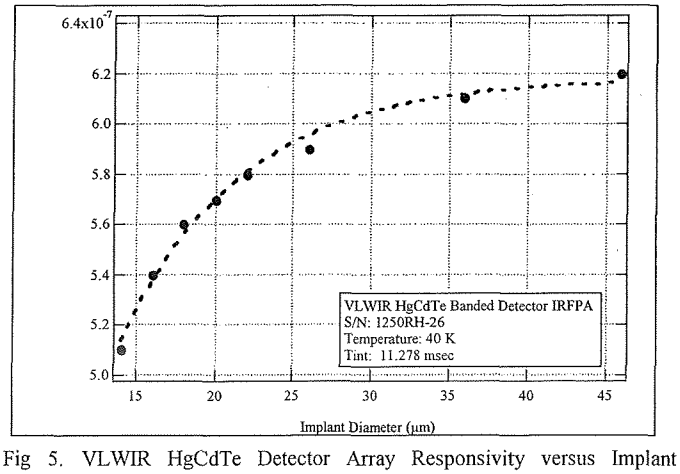

Fig 5. VLWIR HgCdTe Detector Array Responsivity versus Implant Diameter.

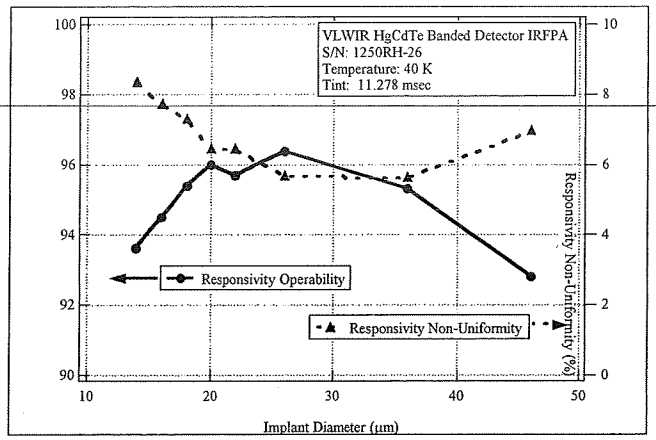

Fig. 6. VLWIR HgCdTe Detector Array Responsivity Operability and Non-Uniformity versus Implant Diameter.

B. Detector Array Proton Radiation Characterization Data

Proton fluence measurements were performed at the Crocker Nuclear Laboratory (CNL) of the University of California, Davis (UC Davis). This proton beam facility is based on a 76" Isochronous Cyclotron that can provide protons with energies up to 68 MeV[16]. For these experiments, the cyclotron was configured to irradiate the detector array at proton energies of 63, 12, and 7 MeV, and the detector array was fully biased and operational at the nominal temperature during irradiation.

1) Responsivity Characteristics at Proton Energy of 63 MeV

The median responsivity of the pixels with eight different implant diameters as a function of proton fluence is shown in Fig. 7. It is evident that all pixel designs exhibit monotonic decrease in responsivity with increasing proton fluence, and that the pixels with the smaller implant diameter exhibit the greatest relative decrease in responsivity with proton fluence. The detector with the largest implant diameter (46 μm) exhibits a responsivity change of -6% at the highest proton fluence of 2.2 x 10^{12} p/cm^2 at 63 MeV. In comparison, the detector with the smallest implant diameter (14 μm) exhibited a responsivity change of -14% at the same proton fluence, which corresponds to a responsivity damage factor of 2.4 x 10^{-20} V/ph/p/cm^2.

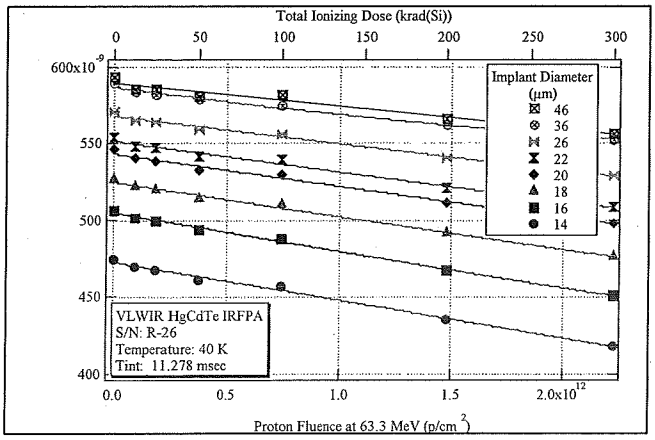

Fig. 7. Median Responsivity versus Proton Fluence at 63 MeV.

As previously outlined, an estimate of the lateral collection length at each proton fluence can be made from these data by plotting the measured responsivity, normalized to the responsivity of the pixel with the largest implant diameter, versus the implant diameter. The lateral collection length can then be estimated by correlating these measured data with the detector finite element model that predicts the detector responsivity as a function of lateral collection length.

This process was followed as shown in Fig. 9 and the lateral collection length was estimated at each proton fluence. The lateral collection length versus proton fluence obtained from this process is shown in Fig. 10. These data show that the lateral collection length decreases by almost a factor of two at the highest proton fluence of 2.2 x 10^{12} p/cm^2 at 63 MeV.

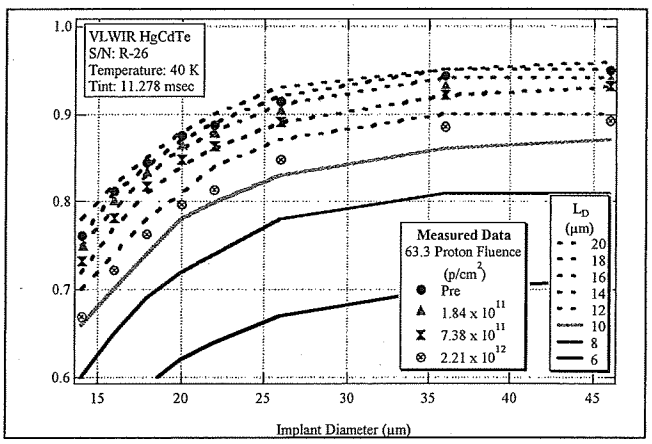

Fig. 9. Relative Responsivity versus Implant Diameter at Different 63 MeV Proton Fluences.

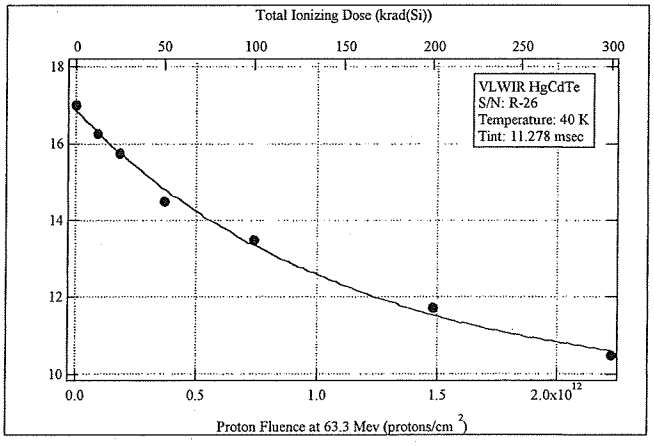

Fig. 10. Lateral collection length versus 63 MeV Proton Fluence.

The inverse of the square of the estimated lateral collection length versus proton fluence is shown in Fig. 11. The slope of this line yields the lateral collection length damage factor, which is 2.5 x 10^{-15} (1/μm^2)/(p/cm^2) at a proton energy of 63 MeV. Recall that this lateral collection length damage factor will be determined as a function of proton energy and will serve as the basis for developing an on-orbit performance model for estimating the change in responsivity of VLWIR HgCdTe detector arrays as a function of on-orbit time.

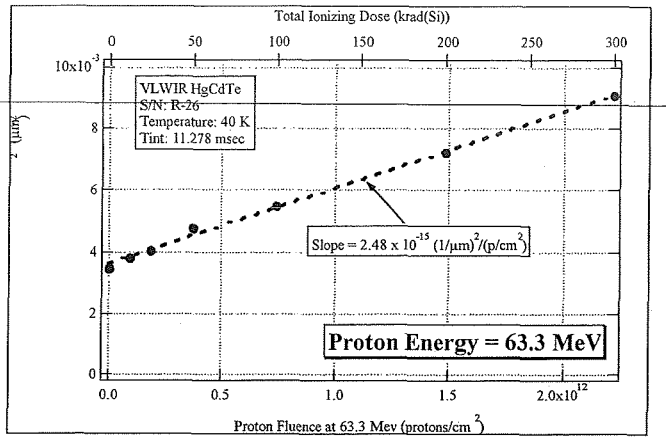

Fig. 11. Lateral collection length Radiation Damage factor Analysis at 63 MeV.

2) Responsivity Characteristics at Proton Energies of 12 and 7 MeV

Similar responsivity measurements were performed on banded detector arrays at proton energies of 12 and 7 MeV. These measurements are summarized in Table 1, which also includes the measured results at proton energy of 63 MeV, that presents the proton measurement energy, the proton fluence at 300 krad(Si), the change in the responsivity at 300 krad(Si) for the 14 μm implant diameter detectors, the computed responsivity damage factor, and the lateral collection length damage factor. This table was generated by analyzing the measured data at each proton energy that consists of determining the change in detector responsivity and the change in lateral collection length as a function of proton fluence.

The measured data at proton energies of 12 and 7 MeV exhibited similar characteristics to the measured data collected at a proton energy of 63 MeV. The measured data at proton energies of 12 and 7 MeV demonstrated that each pixel design exhibited a monotonic decrease in responsivity with increasing proton fluence, and that the pixels with the smaller implant diameter exhibit the greatest relative decrease in responsivity with proton fluence.

Measured data collected at a proton energy of 12 MeV from the smallest implant diameter (14 μm) demonstrates a change in detector responsivity of -12% at a proton fluence of 4.2 x 10^{11} p/cm^2, which corresponds to a responsivity damage factor of 1.2 x 10^{-19} V/ph/p/cm^2. These 12 MeV proton data were further analyzed to determine the lateral collection length as a function of proton fluence. This analysis yields a lateral collection length damage factor of 1.3 x 10^{-14} (1/μm^2)/(p/cm^2).

At 7 MeV, the detector with the 14 μm implant diameter (14 μm) exhibits a change in responsivity of -12% at a proton fluence of 4.2 x 10^{11} p/cm^2, which corresponds to a responsivity damage factor of 1.2 x 10^{-19} V/ph/p/cm^2. Subsequent analysis of these data determined that the lateral collection length damage factor to be 1.3 x 10^{-14} (1/μm^2)/(p/cm^2).

TABLE I
SUMMARY OF MEASUREMENTS VERSUS PROTON FLUENCE

Proton Energy (MeV)	Proton Fluence at 300 krad(Si) (p/cm^2)	Change in 14 μm Implant Diameter Detector Responsivity at 300 krad(Si) Equivalent Proton Fluence (%)	Responsivity Damage Factor (V/ph/p/cm^2)	Lateral Collection Length Damage Factor (1/μm^2)/(p/cm^2)
7	4.2 x 10^{11}	-12%	1.2 x 10^{-19}	1.3 x 10^{-14}
12	6.2 x 10^{11}	-13 %	8.6 x 10^{-20}	7.0 x 10^{-15}
63	2.2 x 10^{12}	-14 %	2.4 x 10^{-20}	2.5 x 10^{-15}

V. ANALYSIS

In this section, the correlation of the measured lateral collection length damage constant and responsivity damage factors to the calculated proton NIEL in HgCdTe is presented. The energy dependence of the NIEL provides a framework for estimating the on orbit performance of these parameters.

This development made two assumptions that required validation to provide confidence in this analysis. The first assumption was that change in detector performance was due to displacement damage and that this change was linear with proton fluence. This first assumption has been validated with the measurement results presented in Section 4. The second assumption was that the lateral collection length and responsivity changes in the detectors has the same energy dependence as NIEL. The second assumption is validated by comparing the energy dependence of the lateral collection length damage factors to the NIEL energy dependence as shown in Fig. 16 and Fig. 17. These measured data show a monotonic decrease in both the lateral collection length damage constant and the responsivity damage factor with energy at the lower proton energies of 7 and 12 MeV. At 63 MeV, the lateral collection length damage factor continues to decrease; but not at the rate predicted by the Coulombic contribution to the NIEL. This is likely due to the increase in the inelastic damage contribution to the total NIEL above proton energies of 30 to 50 MeV. The measured data at 63 MeV does not exactly correspond to the calculated NIEL and if the NIEL curve were used to predict the on-orbit change in detector responsivity, it would provide a conservative estimate of the performance change.

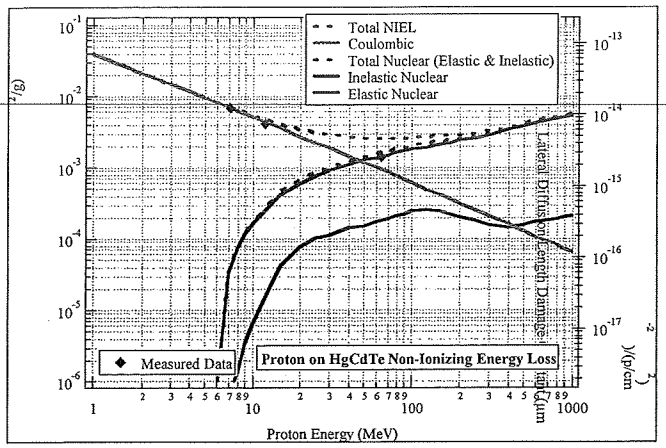

Fig. 16. Energy Dependence of Measured Lateral Collection Length Damage Constant Compared to NIEL Energy Dependence.

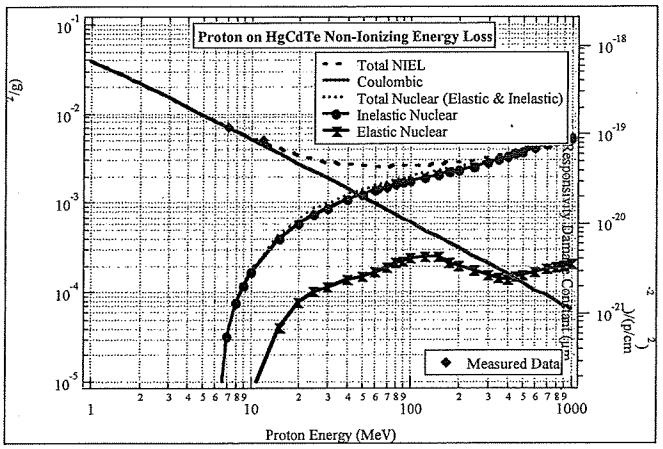

Fig. 17. Energy Dependence of Responsivity Damage Factor Compared to NIEL Energy Dependence.

VI. SUMMARY

This study investigated the change in performance of VLWIR HgCdTe detector arrays in a proton environment. Data have been presented that describe the responsivity characteristics of VLWIR HgCdTe detector arrays as functions of proton fluence at proton energies of 7, 12, and 63 MeV. Measured data show that the VLWIR HgCdTe detectors exhibit a monotonic decrease in responsivity with increasing proton fluence. At each proton fluence, the lateral collection length was estimated by correlating measured data with a detector finite element model that predicts the detector responsivity as a function of lateral collection length. The plot of the inverse of the square of the lateral collection length versus proton fluence was used to determine the lateral collection length damage factor at proton energies of 7, 12, and 63 MeV. The energy dependence of the lateral collection length damage factors shows a monotonic decrease with energy at the lower proton energies of 7 and 12 MeV. At 63 MeV, the lateral collection length damage factor continues to decrease at a rate less than predicted by the Coulombic contribution to the NIEL. This is likely due to the increase in the inelastic damage contribution to the total NIEL above proton energies of 30 to 50 MeV. These measured data validated the assumptions that that displacement damage is linear with proton fluence and that the lateral collection length damage factor in VLWIR HgCdTe detectors has the same energy dependence as NIEL. To further validate this approach, measured data at proton energies between 12 and 63 MeV and also at a proton energy greater than 200 MeV is highly desirable. These results provide the basis for the development of an on-orbit performance model.

REFERENCES

[1] J. Hubbs, D. Arrington, M. Gramer, G. Dole, R. Ramos, "Proton and Total Dose Characterization of VLWIR Focal Plane Arrays that Utilize Micro-Lens Detectors," presented at the 2003 Military Sensing Symposium Specialty Group on Infrared Material and Detectors, Tucson, AZ.

[2] B.C. Fodness, P.W. Marshall, R.A. Reed, T.M. Jordan, J.C. Pickel, I. Jun, M.A. Xapsos, E.A. Burke and R. Ladbury, "*Monte Carlo Treatment of Displacement Damage in Bandgap Engineered HgCdTe Detectors*," Proceedings of the 7th European Conference on Radiation and its Effects on Components and Systems, pp. 479-485, 2003.

[3] J.F. Ziegler, J.P. Biersack and U. Littmark, *The Stopping and Range of Ions in Solids*, Volume 1 of the Stopping and Ranges of Ions in Matter, edited by J.F. Ziegler, Pergamon Press, 1985.

[4] S.R. Messenger, E.A. Burke, M.A. Xapsos, G.P. Summers, R.J. Walters, I. Jun and T.M. Jordan, "*NIEL for Heavy Ions: An Analytical Approach*", *IEEE Trans. on Nucl. Sci.*, Vol. 50, No.6, pp. 1919-1923, December, 2003.

[5] I. Jun, "Effects of secondary particles on the total dose and the displacement damage in space proton environment," *IEEE Trans. on Nucl. Sci.*, Vol. 48, pp. 162-175, February 2001..

[6] "MCNPX User's Manual: Version 2.4.0," LA-CP-02-408, Los Alamos National Lab, September 2002.

[7] I. Jun, M.A. Xapsos, S.R. Messenger, E.A. Burke, R.J. Walters, G.P. Summers and T.M. Jordan, "Proton NonIonizing Energy Loss (NIEL) for device applications," *IEEE Trans. on Nucl. Sci.*, Vol. 50, No.6, pp. 1924-1928, December, 2003.

[8] P. W. Marshall and C. J. Marshall – 1999 IEEE NSREC Short Course.

[9] P. W. Marshall, C. J. Dale and E. A. Burke, "Proton-induced displacement damage distributions and extremes in silicon microvolumes," IEEE Trans. on Nucl. Sci., Vol. 37, pp. 1776-1783, December 1999.

[10] W. McLevige, "HgCdTe Double Layer Planar Heterostructure Detectors for Tactical and Strategic Applications", presented at the 1995 Military Sensing Symposium Specialty Group on Infrared Material and Detectors, Tucson, AZ.

[11] W. McLevige, "Application of Lateral Collection Concepts in LWIR HgCdTe Double Planar Heterostructure Detectors," presented at the 1996 Infrared Information Society Specialty Group on Infrared Material and Detectors, Tucson, AZ.

[12] W. McLevige, " Performance of LWIR HgCdTe Focal Plane Arrays for Low Background 40K Strategic Applications", presented at the 1997Infrared Information Society Specialty Group on Infrared Material and Detectors, Tucson, AZ.

[13] W. McLevige, "Improved Uniformity of Small Area VLWIR HgCdTe Diodes for 40 K Strategic Focal Plane Arrays presented at the 1999 Infrared Information Society Specialty Group on Infrared Material and Detectors, Tucson, AZ.

[14] D. Lee, "Modeling of Optical Response in Graded Absorber Layer Detectors", presented at the 2006 Military Sensing Symposium Specialty Group on Infrared Material and Detectors, Orlando, FL.

[15] D. Lee, Teledyne Imaging Systems, Camarillo, CA, private communication, May, 2006.

[16] C.M. Castaneda, "Crocker Nuclear Laboratory (CNL) Radiation Effects Measurement and Test Facility", 2001 IEEE Radiations Effects Data Workshop, pp 77-81, IEEE (2001).